

# LiB 検査市場に貢献するニコンの X-Ray CT 技術

坂口直史, David Bate, Jan De Geeter, Jos Jans, Ben Morgan

## Nikon's X-Ray CT Technology that Contributes to the LiB Inspection Market

Naoshi SAKAGUCHI, David BATE, Jan DE GEETER, Jos JANS and Ben MORGAN

電気自動車の急速な普及に伴い、バッテリーセルの適切な検査は、バッテリーセルの長期的な性能と安全性を保証するために重要な要素となる。

本稿では、この市場ニーズに応えるニコンの新しい XT H 225 ST 2x X 線コンピューター断層撮影 (CT) システムと、システムに搭載する新機能を紹介する。

最初に、X 線の生成とイメージングの原理、および従来の CT 取得と再構成の手法について説明する。続いて新機能とアプリケーションの紹介を行う。

改良された Rotating.Target2.0により、従来の静的反射ターゲットと比較して、特定の焦点スポットサイズに対して 3 倍の高出力 X 線を得る。独自の Half.TurnCT 取得および再構成アルゴリズムにより、より高速なスキャンが可能になり、X.Tend ヘリカル CT は、高解像度でアーチファクトのないデータを提供する。Auto.FilamentControl はフィラメントの寿命を 2 倍にする。これらすべての新しい 2x の機能は、生産環境でのエンドオブラインテストおよびプロセス制御に X 線 CT を使用するための重要な要件である高速で高品質の CT スキャンを可能にする。

最後に産業用アプリケーションの実例として、リチウムイオン電池セルの高速検査のための XT H 225ST2x システムの使用例について紹介する。

With the rapid adoption of Electrical Vehicles, proper inspection of battery cells is critical to guarantee their long term performance and safety. This paper introduces Nikon's new XT H 225 ST 2x X-ray Computed Tomography (CT) system as well as the new features that come with the system to meet this market need. First the principles of X-ray generation and imaging are explained as well as the traditional CT acquisition and reconstruction techniques. Next, we will introduce new features and applications. The improved Rotating.Target 2.0 makes it possible have a 3 times higher X-ray flux for a given focal spot size compared to a traditional static reflection target. The unique Half.Turn CT acquisition and reconstruction algorithms enables faster scans while X.Tend helical CT provides high-resolution, artefact free data. Auto.Filament Control doubles the lifetime of the filament. All these new 2x features enable fast and high quality CT scans that are a key requirement for the usage of X-ray CT for end-of-line testing and process control in a production environment. Finally, as an example of such an industrial application, the paper discusses the usage of the XT H 225 ST 2x system for fast inspection of Li-Ion battery cells.

**Key words** X 線, コンピュータ断層撮影, リチウムイオンバッテリー, 検査, 生産  
X-ray, Computed Tomography, Lithium-ion battery, inspection, production

## 1 Introduction

Nikon offers a wide range of industry-leading X-ray and Computed Tomography (CT) systems to do non-destructive inspection of parts as small as MEMS up to large castings and this for a wide range of industries including aerospace, automotive, consumer products, electronics and much more. At the heart of these systems are Nikon's X-ray microfocus sources, ranging from 130 kV through to 450 kV, that Nikon X-Tek Systems in Tring (UK) has been developing and

manufacturing in-house since 1986. Unique X-ray source technology such as rotating target, integrated generator and the worlds-only 450 kV microfocus source allow superior image quality across the entire range of systems.

In the early days, X-ray CT was mainly used in Research & Development (R&D) and Failure Analysis. More recently, production quality control teams have seen the benefit of using CT to shorten production set-up time by doing detailed first article inspection and to improve process control by doing systematic end-of-line inspection. In both cases,

a single CT scan enables inspection of internal and external dimensions and reveals defects and assembly issues, all in a non-destructive way and faster than other technologies. The latest trend is to move CT inspection into the production line to catch issues as early as possible. This trend can certainly be seen in the growing market of Li-Ion battery cells that power hybrid and electrical vehicles. Manufacturing quality in this case is important to guarantee long term battery performance and safety.

In the production line, the challenge is to reduce inspection cycle times as much as possible without compromising on data quality. The remainder of the paper will explain how Nikon has responded to this challenge by further improving source performance and implementing innovative CT scanning techniques and reconstruction algorithms which resulted in the new XT H 225 ST 2x X-ray CT system.

## 2 Technology Background

### 2.1. Principle of X-ray Imaging

X-rays are a form of electromagnetic radiation, just like visible light, but compared to many other types of radiation, X-rays are more energetic. An X-ray photon can be hundreds or thousands of times more energetic than a photon of visible light, see Fig. 1.

Wilhelm Roentgen first described X-rays in 1895, an achievement for which he was awarded the very first Nobel Prize in Physics. During World War I, X-rays were already being used for medical purposes.

Most of the X-rays in the universe arise when highly excited atoms decay back to their ground state configuration. For example, if an electron is removed from the inner shell orbitals of an atom — perhaps by a collision with something — then the atom will emit an X-ray photon as it returns to its equilibrium state.

Another common source of X-rays is from a process called “bremsstrahlung”, which is German for “braking radiation.” X-rays are emitted when a highly energetic beam of charged particles such as electrons is rapidly decelerated — because it runs into a metal target, for example.

In medical and industrial X-ray sources, a beam of energetic electrons is focused onto a target, usually a piece of Tungsten. As the electrons are decelerated, this generates bremsstrahlung X-rays. In addition, the incoming electrons can collide with a Tungsten atom and knock an electron out from its inner orbit. This kind of device actually produces X-rays by both mechanisms simultaneously.

The high energy of the X-rays combined with their inter-

actions with the electron cloud in the atoms means that X-rays can penetrate significant amounts of material; the exact length depends on density and atomic number and broadly falls off as either increases. The X-rays that pass through the material (as well as those scattered) can then be detected. Originally this was done using film but over the years a number of electronic means have become available.

Today the most common type of detector in industrial X-ray is the flat panel detector, that consists of a scintillator material (most often Caesium Iodide (CI) or Gadolinium Oxysulphide (GdOx)) that converts the incident X-rays into light. These scintillators sit on top of a layer of photo diodes which convert the light generated into a 2D image which is read out to a computer.

The key equation in X-ray image formation is the Beer Lambert law which describes how the intensity of the detected X-rays falls off with the thickness of material:

$$I = I_0 e^{-\mu t} \quad (1)$$

The equation (1) is true for a monochromatic beam traversing a uniform material with attenuation coefficient  $\mu$ , the equation can be extended to polychromatic beams as found in typical microfocuss sources and to multiple materials.

### Electromagnetic Spectrum

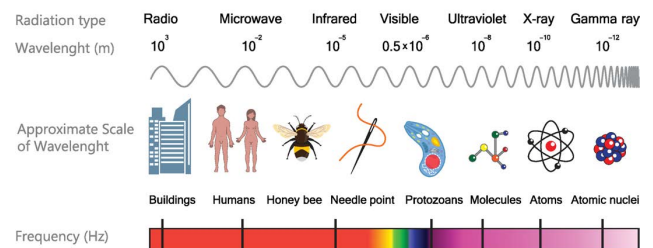


Fig. 1 Overview of the Electromagnetic spectrum showing the place of X-rays within it.

When an image is collected the values of  $I_0$  and  $I$  can be measured before and after the sample is introduced. This in turn will allow calculation of the attenuation along that path, this will be important later when we discuss Computed Tomography.

### 2.2. Features of Microfocus X-ray Sources

There are several different types of X-ray sources. Of most use in industry are the Mini-focus tube (X-ray focal spot size  $> 100$  microns) and the Microfocus tube (focal spot size  $< 100$  microns, typically  $< 10$  micron at best). Within each type there are two competing construction methods: sealed tube in which the source is put under

vacuum and then sealed and runs in a sealed state until failure, when it is replaced. Next to this, there is or the open tube, in which the source can be vented to air and the filament or other failed parts replaced, giving it an unlimited lifetime.

The customer will choose the type that best matches their sample and imaging needs.

A typical Microfocus tube will consist of the following elements, see Fig. 2.

- 1) A high voltage receptacle to allow the high voltage (typically around 200 kV) to be delivered
- 2) An electron source, often a heated Tungsten hairpin
- 3) A cathode/anode assembly causing electrons to be extracted from the filament and accelerated
- 4) A drift space with steering coils to make sure the beam passes through the centre of the lens
- 5) An electromagnetic lens to focus the beam
- 6) A metallic target of a suitable material to generate X-rays (typically Tungsten).

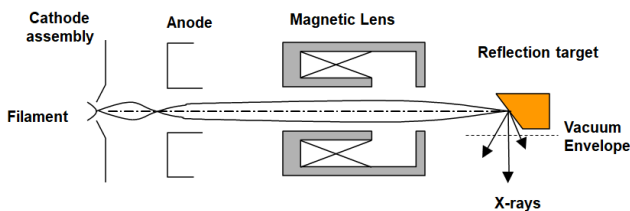


Fig. 2 Outline of a microfocus source.

The biggest remaining variation is on the type of target used, there are two axes:

a) Stationary or Rotating

A stationary target is fixed in place; it has the advantage that with no moving parts it can give a stable source. The rotating target allows a much higher power density (electrons per unit area) which leads to a much higher X-ray flux for a given spot size.

b) Reflection or Transmission

A reflection target sends the beam of electrons into a large block of the target material and the X-rays used are those that come back out of the target (i.e. are 'reflected' back), it is easier to cool but allows the electrons to spread in the target so limits the X-ray source size. A transmission target is a thin film where the electrons hit one side and the X-rays are taken off the other side (i.e. they are 'transmitted'). This enables a smaller spot to be achieved but is harder to cool so can only be used at lower powers.

### 2.3. Introduction to Computed Tomography and Reconstruction Algorithms

By combining 2D radiographs from an object taken from different directions, a 3D representation of the object can be created. The most commonly used Computed Tomography algorithm is Circular FDK CT.

In this mode individual images (call projections) are taken while the object rotates 360 degrees in the X-ray beams, see Fig. 3. By application of the Radon transform to the attenuation found from the images the data can be back projected into the 3D volume of the sample.

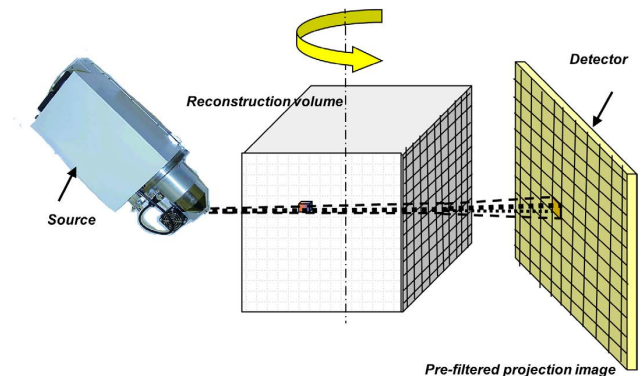


Fig. 3 Schematic of CT data acquisition.

It was found that if the attenuation was simply back projected then the resulting image was blurred and so a filtering step was introduced to form Filtered Back Projection, the most commonly used algorithm for this is the FDK algorithm from Feldkamp et al [1].

The FDK algorithm is imperfect and can lead to errors in the final volume Below is a short list of the most common errors:

- 1) Off axis errors – the algorithm is only fully correct on the central horizontal slice that passes through the focal spot of the source. As the angle to the object increases there is a loss of information and this introduces off axis errors, usually a blurring or drop in SNR.
- 2) Field of view – the algorithm relies on the whole object being contained with the cone subtended by the detector. If parts of the object are outside this cone then errors will occur; usually this introduces a bright ring.
- 3) Beam hardening – as the X-ray beam is polychromatic and the Beer Lambert law is monochromatic there is a mismatch. This is made worse as attenuation changes with kV but only the integrated intensity is measured, which leads to a non-linear value of the attenuation. There are extensions of FDK that allow for correction of this effect for single and multiple materials.

### 3 New XT H 225 ST 2x features

#### 3.1. Introduction of the XT H 225 ST 2x System

The XT H 225 ST 2x standard system is equipped with a 225 kV source with Rotating.Target 2.0 with a focal spot size of  $10\ \mu\text{m} < 30\ \text{W}$  and a maximum focal spot size of  $160\ \mu\text{m}$  at 450 W. The 8.3 MP flat panel has a pixel size of  $150\ \mu\text{m}$ . Fig. 4 is a system picture.



Fig. 4 Picture of the XT H 225 ST 2x system.

#### 3.2. Improved Rotating.Target 2.0

One ongoing issue with all X-ray CT is that the image quality of the result is directly related to the amount of X-ray flux collected. This means that for a given flux a longer scan will have better image quality than a shorter scan.

In order to improve the quality of short scans the 2x system incorporates a Rotating.Target 2.0. Such a target consists of a rotating disc with a sloped surface and Tungsten coating. As 99% of the power of the electrons hitting the target is converted into heat and only 1% into X-rays, focusing the electron beam on a very small area of the target will melt the target. With the rotating target, this focal spot is not a single spot but a much larger circular area that can be cooled much more efficiently through a combination of water cooling and radiative cooling. This approach allows a much higher electron power density on the target. This can then be used to either have a much higher flux at the same spot size or a much smaller spot size at a given flux. For the 2x the main use is the former, where the X-ray flux can be increased by a factor of about 3x from the static reflection target, this can then shorten the time taken for a given quality by the same factor.

#### 3.3. Auto.Filament Control Doubles the Life of Filaments

High-resolution microfocus X-rays start with electrons emitted from a thin filament that has to be replaced periodically due to wear. Less frequent changing of the filament is

desirable, as it means that system availability is higher. Long-life filaments are available but they are thicker, so the high resolution nature of the microfocus X-rays is lost. With the XT H 225 ST 2x, the user no longer has to choose between high-resolution and long-life filaments. Auto.Filament Control intelligently controls the X-ray source to double the lifetime of the filament and increase system availability.

Auto.Filament Control carefully controls the current through the filament to optimize its lifetime. The current through the filament causes the filament to warm up, which allows electrons to be emitted which are then accelerated and focused on the X-ray target to generate X-rays. Increasing the current through the filament will increase the temperature and the amounts of electrons produced, up to a point where this saturates, and further increasing the current will not significantly increase the amounts of electrons emitted. This function has the general shape of a logistic function, or S-shaped function. The challenge is to determine at every point in time, and for every combination of desired beam current and energy ( $\mu\text{A}$ ,  $\text{kV}$ ) where this saturation point or “knee” point is. Whilst this needed to be identified by an operator before, this is now fully automated in the XT H 225 ST 2x. After the installation of a new filament, with one click of a button, the system automatically identifies this knee point in the filament demand curve for every combination of beam current and energy ( $\mu\text{A}$ ,  $\text{kV}$ ), see Fig. 5.

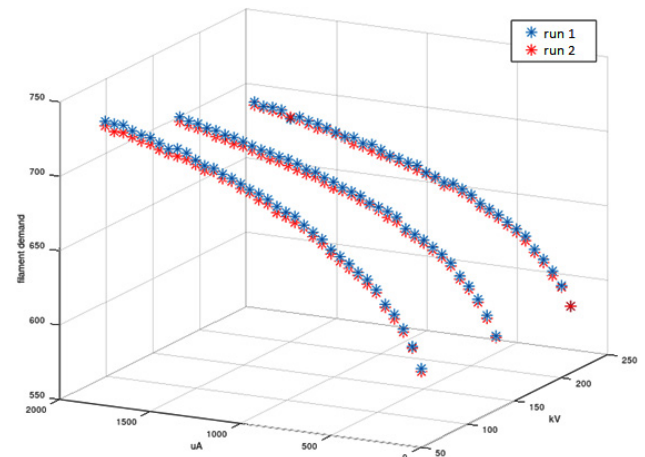


Fig. 5 Identified filament demand map, showing the knee point in the filament demand curve (arbitrary units from high-voltage generator) as a function of desired beam current ( $\mu\text{A}$ ) and energy ( $\text{kV}$ ). This graph shows two repeated runs with several days in between, showing that the identified values are stable and repeatable.

Experiments have shown that the map shown in Fig. 5 is stable over time. However, as the filament starts to wear, and

other parameters in the source vary slightly, the map becomes slightly offset, but the shape remains the same. Therefore, the XT H 225 ST 2x periodically identifies this offset without further operator intervention, achieving the optimal lifetime of the filament all the way to the end when it will finally break. This way, this new Auto.Filament Control function has proven to extend the lifetime of filaments by a factor of 2 compared to filaments that are manually tuned.

### 3.4. X.Tend, Error-Free Helical CT Reconstruction

In the above discussion of FDK one of the errors was that the equations were only accurate on the central plane. Helical CT was devised to address this weakness. There are a number of different helical algorithms but they all work on the same basic principle. By moving the sample vertically as the sample rotates the angles at which the object is seen vary continuously changing the volume of correct slices.

Many helical algorithms work to smear out the errors over the whole volume, however, there are a few algorithms that are exact, one of which is the Katsevich algorithm [2], [3], [4] which Nikon uses for its helical CT reconstruction, this uses a smaller region of the detector during the scan combined with an algorithm to arrive at an accurate reconstruction which does not contain any errors due to the reconstruction process.

Another benefit of helical CT is that for taller samples, the whole part does not need to be in the field-of-view of the flat panel. In practice this means that the part can be brought closer to the source and can be scanned at higher magnification, see Fig. 6.

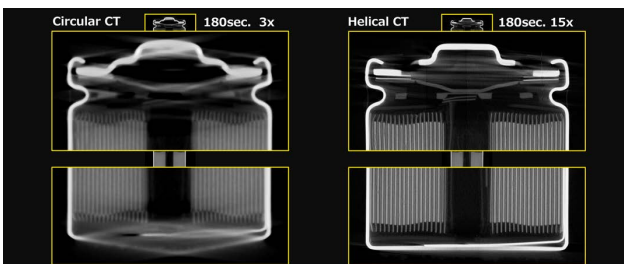


Fig. 6 Cylindrical battery cell on the left scanned with circular CT at 3 times magnification and scanned on the right hand side with X.Tend helical CT at 15 times magnification.

### 3.5. Half.Turn CT Doubling the Speed of the Acquisition

The new XT H 225 ST 2x system doubles the speed of the acquisition compared to a similar acquisition on the XT H 225 ST, without giving in on data quality. This is achieved by a more sensitive detector, in combination with the new Half.Turn CT acquisition and reconstruction software.

The duration of a CT acquisition is shown as (2)

$$T_a = \frac{\Delta\theta * R_\theta}{F} \quad (2)$$

where  $T_a$  is the time of the acquisition in (sec),  $\Delta\theta$  is the angular range of the scan (rad),  $R_\theta$  is the desired angular resolution (frames/rad) and  $F$  is the frame rate of the detector (frames/sec).

$R_\theta$  is usually optimized based on the resolution of the detector, such that  $\frac{r}{R_\theta}$  is more or less equal to the pixel size of the imager, where  $r$  is the radius of the object begin scanned. Reducing  $R_\theta$  will reduce the resolution of the reconstructed volume, and will increase motion blur, which is undesirable.

$F$  is limited by the maximum frame rate of the detector, and its sensitivity. The Varex XRD4343CT panel is more sensitive than the Varex PE1621EHS used before. Running the XRD4343CT detector at 15 frames per second gives a similar quality image as the PE1621EHS detector at 11 frames per second. Further increasing the frame rate is not possible, as 15 frames per second is the maximum speed of the detector in full frame mode.

Therefore, if we want to double the speed of the acquisition without compromising the resolution while the imager is already at full frame rate, then the only remaining parameter we can play with is  $\Delta\theta$ , the angular range of the scan. For regular CT scans,  $\Delta\theta$  is  $2^*\pi$  or a full turn. However, is that really needed? In case we have a system with a parallel X-ray beam, the image at angle  $\theta$  should contain the exact same information as the image at angle  $\theta + \pi$ . So,  $\Delta\theta = \pi$  should give the same resolution of the reconstructed volume, albeit with a lower signal to noise ratio compared to the full turn scan as we capture only half the number of images.

In case of a cone beam,  $\Delta\theta$  needs to be larger than  $\pi$  because of the cone beam opening angle. For every point on the scanned object to be seen by rays in the whole range from 0 to  $\pi$ , the rotate stage needs to turn over an angular range  $\Delta\theta = \pi + \alpha$ , where  $\alpha$  is the cone beam opening angle. Fig. 7 explains this.

This scan over a range  $\Delta\theta = \pi + \alpha$  with a cone beam system presents a particular challenge to reconstruction. It is well known that straightforward reconstruction of such an acquisition with standard Filtered Back Projection introduces artefacts. The origin of these artefacts is the "asymmetry" in the dataset caused by the cone beam. As Fig. 7 shows, some parts of the objects are penetrated by more rays than others, and hence more information is available about the parts closer to the source. The new Half.Turn CT reconstruction solves this unfairness, and provides a reconstruction of the

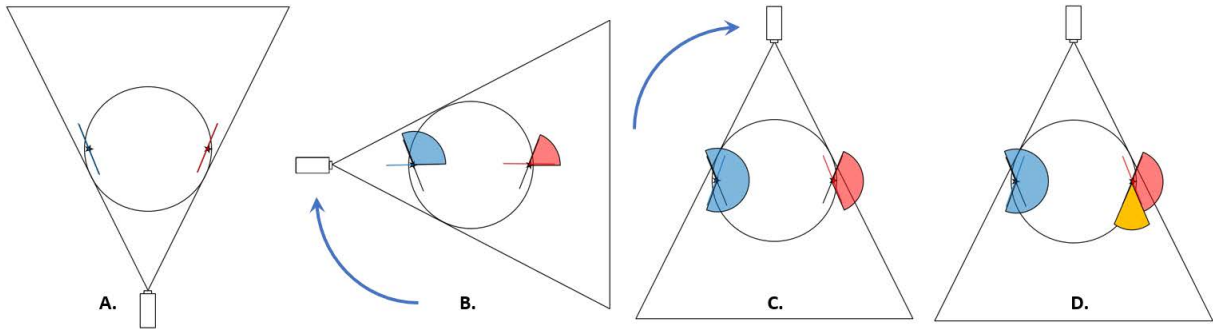


Fig. 7 For every region of the object to be seen by rays in a range of  $0$  to  $\pi$ , the stage needs to rotate over an angle of  $\pi +$  cone beam angle  $\alpha$ . (A) Consider regions at opposite ends of the sample. The beam passes through these at an angle. (B) After  $90^\circ$  of rotation, the blue feature receives a wider angular coverage for the same rotation. The red feature on the opposite end receives less coverage. (C). After  $180^\circ$  of rotation, the blue feature has over  $180^\circ$  of coverage, and therefore has more than enough projection data to allow reconstruction. The red feature, however, has insufficient coverage. It will be missing detail at angles which have not been covered. (D) We must therefore rotate further to cover this missing angle. This additional angle is equal to the cone beam angle.

same quality as a full turn CT, without adding noticeable computation time. Fig. 8 shows that the quality of the new Half.Turn CT reconstruction is comparable to that of a standard FDK reconstruction of a full turn scan of the same object, while needing only about half of the images.

Fig. 9 compares the acquisition time of 2 CT acquisitions that produce equivalent data quality, one full turn scan on the XT H 225 ST, and one Half.Turn CT scan on the new XT H 225 2x system. The doubling of the speed is achieved through a combination of a more sensitive detector, allowing it to run at full frame rate of 15 frames per second, and the new Half.Turn CT reconstruction providing a reconstruction quality that is similar to that of the full turn scan.

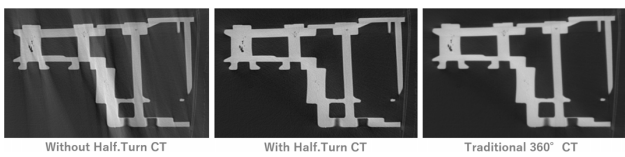


Fig. 8 Comparison between a Half.Turn CT acquisition reconstructed with standard FDK (left), the same acquisition reconstructed with the new Half.Turn CT reconstruction (middle), and a full turn CT acquisition reconstructed with standard FDK (right). The left figure clearly shows artefacts, while the quality of the Half.Turn CT reconstruction (middle) is comparable to that of a standard FDK reconstruction of a full turn scan (right).

## 4 2x improvements applied to Li-Ion battery cell inspection

For Li-Ion batteries, defects like inclusion of foreign particles, electrode delamination and incorrect anode overhang can be disastrous for their long-term performance and safe

	XT H 225 ST	XT H 225 ST & Half.Turn CT
Detector panel	PE1621EHS	XRD4343CT
Beam energy	165kV	180kV
Beam current	236 $\mu$ A	222 $\mu$ A
Power	39W	40W
Exposure time	88ms	67ms
Projections per full turn	3141	3800
Number of projections	3141	2126
<b>Acquisition time</b>	<b>4m52s</b>	<b>2m26s</b>

Fig. 9 Comparison of the acquisition time between a full turn CT acquisition on a XT H 225 ST, and a Half.Turn CT scan on the new XT H 225 ST 2x system. Acquisition speed is exactly doubled by the use of a more sensitive detector, combined with the new Half.Turn CT reconstruction.

operation. That's why it is important to catch these issues at the end of the line or even better, during the assembly process. As this is high volume production, cycle time is key without compromising on image quality.

The examples below show how the combination of Rotating.Target 2.0, the latest flat panel technology and Half.Turn CT allows users to drastically reduce scan time. See Fig. 10-14.

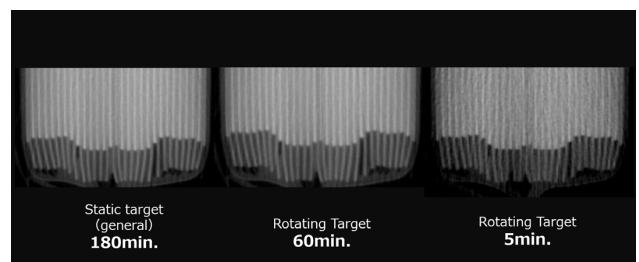


Fig. 10 Comparison of image quality of battery anode overhang using Rotating.Target 2.0 and ever shorter scan times.

Fig. 10 is a CT image of the anode overhang of the electrode stack of a Li-Ion battery cell, demonstrating the change of image quality when the scan time is shortened by using a Rotating.Target 2.0. The image on the left was acquired using a standard static reflection target; for the center image a Rotating.Target 2.0 was used and the scan time was reduced with a factor 3, while for the image on the right the scan time was further reduced with a factor 12. Even in the last case where the scan time is 36 times shorter than the original scan time, the image maintains sufficient resolution for proper overhang analysis.

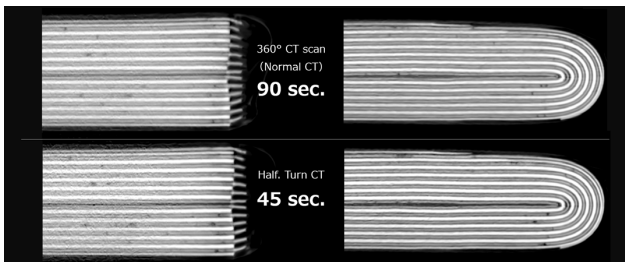


Fig. 11 Comparison of image quality using traditional circular CT versus Half.Turn CT.

Fig. 11 is a comparison of the image acquired in 90 seconds using traditional circular CT and the image acquired in 45 seconds using Half.Turn CT. In the last case, almost equivalent image quality is obtained in half of the time needed to scan the battery cell.

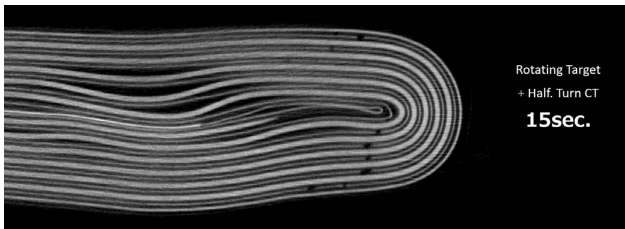


Fig. 12 Delamination and deformation of battery electrodes are clearly visible in a 15 seconds scan.

During the winding or stacking process of the anode, separator and cathode and during the further assembly process of the battery cell, delamination or deformation of the electrodes can happen. Fig. 12 is a CT image showing electrode delamination and deformation inside such a Li-Ion battery cell. The data set is acquired in just 15 seconds using Rotating Target 2.0 and Half.Turn CT.

Fig. 13 shows a CT image that captures the crack in a battery electrode. Cracks are a critical internal defect that can be introduced during the slitting process. A normal CT scan takes 45 seconds to acquire, but Nikon has made it possible to acquire it in just 15 seconds with Rotating.Target 2.0 and

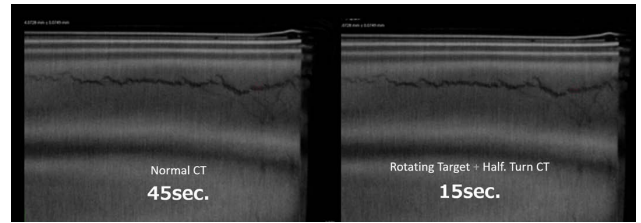


Fig. 13 Visualisation of an electrode crack in a 15 second CT scan.

Half.Turn CT. Almost equivalent image quality is obtained with a 3 times shorter scan.

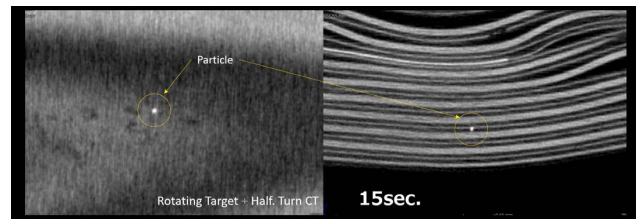


Fig. 14 Visualisation of foreign particle in a Li-Ion battery cell.

During the whole process from winding or stacking of electrodes up to the sealing of the battery cell, foreign particles can be caught inside the cell. Also the welds that connect the anode and cathode to the external battery terminal can include voids that result in bad electrical conductivity.

On Fig. 14 some foreign particles can be clearly seen on the CT image that was acquired in only 15 seconds using Rotating.Target 2.0 and Half.Turn CT.

## 5 Conclusion

In this paper the new and improved features of Nikon's latest XT H 225 ST 2x industrial CT system were explained. These include Auto.Filament Control, that doubles filament lifetime, Half.Turn CT and X.Tend helical acquisition and reconstruction algorithms and the improved 225 kV Rotating.Target 2.0 X-ray source. It was shown how these features increase the scan speed of the system while maintaining or improving the image quality.

Fast scans and reliable analysis are a key requirement to enable the usage of X-ray CT for end-of-line testing and process control in a production environment. As an example of such an industrial application, the paper discusses the usage of the XT H 225 ST 2x system for fast inspection of Li-Ion battery cells. The results show that critical defects like incorrect anode overhang, electrode delamination and foreign particle inclusions can be detected in scans that take no more than 15 seconds.

This makes Nikon's X-ray CT system with its unique X-ray source and software technology, particularly suited for the inspection of Li-Ion battery cells, of which production volumes are increasing rapidly with the growing demand for Electric Vehicles. Also the mass production of other components like Plastic Injection Moulded connectors and small castings, that are widely used in Electrical Vehicles, will benefit from these advances in X-ray CT inspection.

### References

---

[1] Feldkamp, L.A, David. L.C, Kress, J.W., "Practical cone

beam algorithm," *Journal of the Optical Society of America A*, vol. 1, no. 6, p. 612-619, 1984.

[2] A. Katsevich, "Exact Filtered Back Projection (FBP) algorithm for spiral Computer Tomography," US Patent 6,574,299, Jun. 3, 2003.

[3] A. Katsevich, "Theoretically exact Filtered Back Projection-type inversion algorithm for spiral cone-beam," *SIAM J. Appl. Math.*, vol. 62, no. 6, p. 2012-2026, 2002.

[4] A. Katsevich, "An improved exact Filtered Back Projection algorithm for spiral Computed Tomography," *Adv. Appl. Math.*, vol. 32, no. 4, p. 681-697, 2004.

---

坂口直史 Naoshi SAKAGUCHI  
産業機器事業部 マーケティング部  
Global Marketing Department  
Industrial Metrology Business Unit

David BATE  
Nikon X-TEK Systems Ltd

Jan DE GEETER  
Nikon Metrology NV

Jos JANS  
Nikon Metrology NV

Ben MORGAN  
Nikon Metrology NV



坂口直史  
Naoshi SAKAGUCHI



David BATE



Jan DE GEETER



Jos JANS



Ben MORGAN